Molecular Spin-Flip Loss and a Dual Quadrupole Trap

David Reens,* Hao Wu,* Tim Langen,† and Jun Ye
JILA, National Institute of Standards and Technology and the University of Colorado and Department of Physics, University of Colorado, Boulder, Colorado 80309-0440, USA
(Dated: October 17, 2017)

Doubly dipolar molecules exhibit complex internal spin-dynamics when electric and magnetic fields are both applied. Near magnetic trap minima, these spin-dynamics lead to enhancements in Majorana spin-flip transitions by many orders of magnitude relative to atoms, and are thus an important obstacle for progress in molecule trapping and cooling. We conclusively demonstrate and address this with OH molecules in a trap geometry where spin-flip losses can be tuned from over 200 s^{-1} to below our 2 s^{-1} vacuum limited loss rate with only a simple external bias coil and with minimal impact on trap depth and gradient.

The ultracold regime extends toward molecules on many fronts [1]. Feshbach molecules at the BEC-BCS crossover have been studied [2–5], ground state alkali dimers continue to progress [6–14], and KRb polar molecules have reached quantum degeneracy in an optical lattice [15]. Recently developed laser cooling strategies are tackling certain nearly vibrationally diagonal molecules [16–21]. A diverse array of alternative strategies have succeeded on other molecules [22–29], including those now enabling molecular collision studies [30–33]. Many of these directly cooled molecules will require secondary strategies like evaporation or sympathetic cooling to make further gains in phase space density [34–36]. They also may face a familiar challenge: spin flip loss near the zero of a magnetic trap, but dramatically enhanced for doubly dipolar molecules, relative to atoms, due to their internal spin dynamics in mixed electric and magnetic fields.

Spin flips were directly observed for magnetically trapped atoms near 50 μK and overcome with a time-orbiting potential trap [37] or an optically plugged trap [38], enabling the first production of Bose-Einstein condensates. Non-laser-based molecular cooling experiments begin at modest temperatures and require trap strengths typically only attained with quadrupole fields [22, 39–42]. In the 2 T/cm magnetic quadrupole used in our previous studies of hydroxyl radicals (OH) [35], spin-flips should not have had a significant influence until the μK regime, but the application of electric field changes this. Electric fields applied to magnetically trapped dipolar species offer interesting opportunities to study anisotropic collisions and quantum chemistry [43]. They can also be useful for control over state purity [44]. But the electric field can also dramatically enhance spin-flip losses, due to internal spin-dynamics that we corroborate with direct experimental evidence for the first time in the present work. We achieve this with a novel trap geometry that also allows complete removal of the loss with minimal sacrifice of trap strength.

The internal spin-dynamics leading to spin-flip enhancement are subtle, having eluded two previous investigations: In Ref. [45] the analogues of atomic spin-flip loss for molecules in mixed fields were modeled. It was concluded that no significant loss enhancement due to electric field would be evident. However, this conclusion holds only for the approximate Hamiltonian used in that study, not more generally. In Ref. [46] it was

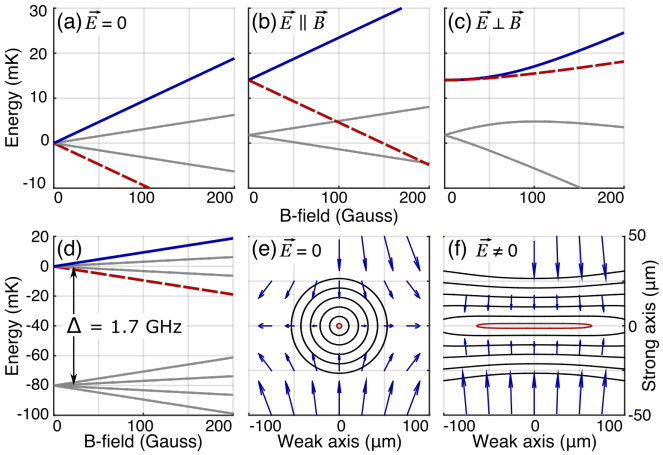

FIG. 1. A uniform electric field, added to magnetically trapped molecules for dipolar studies or other purposes, can lead to spin-flip losses. Four Zeeman split lines in OH's $X^2\Pi_{3/2}$ manifold are shown (a-c), with the doubly stretched state in blue and its spin-flip partner in dashed red. These states are shown with no electric field (a), with $|\vec{E}| = 150$ V/cm and $\vec{E} \parallel \vec{B}$ (b), and with $\vec{E} \perp \vec{B}$ (c). Note the vastly reduced red-blue splitting in the latter case. The ground state consists of two parities and four m states each, usually labeled $|\text{parity} = f, e;\ m = \pm 1/2, \pm 3/2\rangle$. The negative parity, electrically strong field seeking manifold sits Δ below (d). The application of electric field generally drives these parities further apart, but within each parity manifold the exact modification depends on the relative field orientations (b-c). In panels (e-f), energy splitting contours are shown every 40 MHz near the zero of a 2 T/cm magnetic quadrupole trap for OH molecules [44] with $\vec{E} = 0$ (e), and with uniform $E = 150$ V/cm along the strong axis of the quadrupole (f). The vectors are $d_{\text{eff}}\vec{E} + \text{sign}(\vec{E} \cdot \vec{B})\mu_{\text{eff}}\vec{B}$, the proper quantization axis for well-trapped molecules as described in the text. Note the drastic widening of the lowest contour (red), the culprit for molecular spin-flip loss enhancement.

correctly noted that Hund's case (a) molecules maintain a quantization axis in mixed fields. The states of the molecule were shown to align with one of the two quantization axes given by the vectors $d_{\rm eff}\vec{E} \pm \mu_{\rm eff}\vec{B}$ [47], $\mu_{\rm eff}$ and $d_{\rm eff}$ the effective dipole moments of the molecule in uncombined fields. The key idea is that Hund's case (a) molecules have both dipole moments fixed to their internuclear axis, so that in the molecular frame, the energy shifts from the two fields combine like vectors. It was asserted that this would maintain quantization near the zero of a quadrupole trap and avoid spin-flip loss, but as we now describe, the loss is actually enhanced.

We begin with an intuitive picture. In order to remain well trapped in combined fields, a molecule must remain weak field seeking with respect to both fields, i.e. doubly stretched. This means that its quantization axis, which is proportional to the field induced energy shift of the molecule, should have maximal length. In a geometry where the fields are continuously rotating, the maximal quantization axis can be either of $d_{\rm eff}\vec{E} \pm \mu_{\rm eff}\vec{B}$, depending on whether the fields are oriented closer to parallel or antiparallel. Consider a molecule in a magnetic quadrupole trap with a uniform electric field. This trap has two hemispheres, a parallel hemisphere where the fields are closer to parallel, and vice versa. The hemispheres are separated by a plane where $\vec{E} \perp \vec{B}$, which intersects the trap center. Now suppose a molecule in the doubly stretched state begins in the parallel hemisphere. Its quantization axis must be the field sum $d_{\rm eff}\vec{E} + \mu_{\rm eff}\vec{B}$. If its trajectory carries it near the trap center where the magnetic field is small, the electric field does indeed maintain the quantization axis. However when the molecule enters the antiparallel hemisphere, the magnitude of the quantization axis now decreases with increasing magnetic field. This molecule has therefore spin-flipped from the doubly stretched state to a magnetically strong field seeking state. These states are degenerate in the plane where $\vec{E} \perp \vec{B}$, leading to loss.

This intuition agrees with a more rigorous analysis of the energy splitting G between the trapped state and its spin-flip partner. By diagonalizing the approximate eight state ground molecular Hamiltonian for OH, subtracting the relevant state energies and Taylor expanding, we find:

$$G(\mathcal{B}_\perp, \mathcal{B}_{||}, \mathcal{E}) = 2\mathcal{B}_{||} + 4.3{\cdot}\mathcal{B}_\perp^3 \frac{\Delta^2}{\mathcal{E}^4} + \mathcal{O}(\mathcal{B}_{||}^2, \mathcal{B}_\perp^4) \qquad (1)$$

Here $\mathcal{B}_{\perp,||} = \mu_{\rm eff}\vec{B}\cdot\hat{e}_{\perp,||}$, where $\hat{e}$ is the unit vector in the labeled direction relative to the electric field. $\mathcal{E} = |d_{\rm eff}\vec{E}|$, Δ is the lambda doubling (see Fig. 1d). The relevant splitting is not quite zero where $\vec{E} \perp \vec{B}$ and $B_{||} = 0$ thanks to Δ, but nonetheless reaches a deep minimum; the remaining Zeeman splitting is reduced from linear to cubic in magnetic field (Fig. 1). This Zeeman splitting suppression is in fact a known phenomenon in the precision measurement community [48, 49], and experimentalists have exploited it to suppress the influence of magnetic fields in electron EDM measurements. However, in the case of applying mixed fields during trapping, this suppression is not beneficial but rather detrimental.

TABLE I. Enhancements (η) and loss rates (γ) for OH with typical applied fields. Zero field values are equivalent to traditional spin-flip loss. Electric field is required during evaporation and spectroscopy to open avoided crossings [35, 44], or applied to polarize the molecules and study collisions [43].

E (V/cm)	55 mK		5 mK		Purpose
	η	$\gamma\,(s^{-1})$	η	$\gamma\,(s^{-1})$	
0	1	0.02	1	1.3	Zero Field
300	5	0.1	9	11	Evaporation
550	17	0.3	40	50	Spectroscopy
3000	1000	19	1600	2000	Polarizing

To deduce the effect of this loss plane on the ensemble, we consider molecular trajectories in light of the Landau Zener formula:

$$P_{\rm hop} = e^{-\pi\kappa^2/2\hbar\dot{G}}, \qquad (2)$$

which relates the probability of diabatically hopping between two states $P_{\rm hop}$ to their energetic coupling κ and their rate of approach $\dot{G} = v_z dG/dz$. Here z and v_z are normal to the $\vec{E} \perp \vec{B}$ plane, and we neglect the components of $\dot{G}$ due to the other coordinates since from Eqn. 1 it is clear that G grows predominately in one direction. We can also set κ to the minimum energy gap along the trajectory, which is found in the plane. This facilitates direct numerical computation of the loss rate (γ) by integrating the molecule flux through the plane for a thermal distribution, weighted by the hopping probability. See Eqn. 2 in Sec. A of the Supplementary [50] for the full expression. We perform these integrations for OH over the velocity distribution in a 2 T/cm magnetic quadrupole [39] under various electric fields in Tab. I.

We have also developed an algebraic scaling law, which yields the electric field induced loss enhancement factor

$$\eta = \frac{3}{11}\left(\frac{d_{\rm eff}E}{\sqrt{\kappa\Delta}}\right)^{8/3}, \qquad (3)$$

see Sec. C of [50] for the full derivation. Here κ represents a characteristic energy scale for spin-flips that can be derived by setting $P_{\rm hop} = 1/e$ in Eqn. 2 and using a typical value of v_z. This means that for electric fields with $d_{\rm eff}E > \sqrt{\kappa\Delta}$, the loss enhancement is almost cubic with electric field. Crucially, it is not Δ that sets the relevant scale, as one might naively suppose given that this is the energy beyond which the Stark effect is linear and the molecule is polarized. Instead it is $\sqrt{\kappa\Delta}$, which is in general much smaller; $\kappa = 5$ MHz for OH in our trap, while $\Delta = 1.7$ GHz.

Returning to the numerical approach, the direct integration of flux is a key improvement relative to our

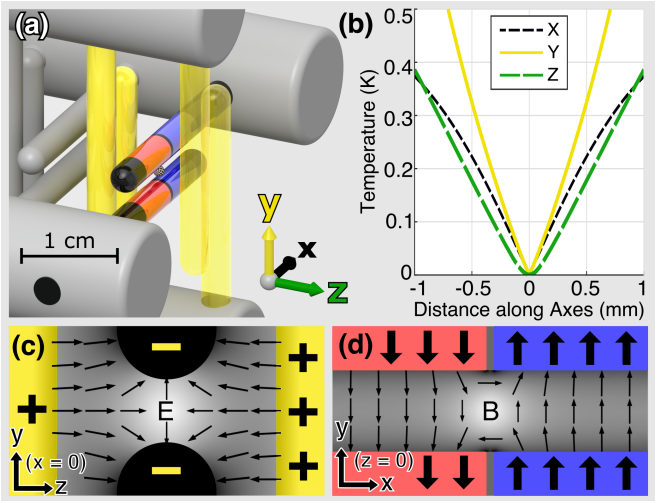

FIG. 2. The last six pins of our Stark decelerator [39] form the trap (a), which is 0.45 K deep with trap frequency $\nu \approx 4$ kHz (b). Along y the trap is bounded by the 2 mm pin spacing. The yellow pins are positively charged and the central pin pair negatively, which forms a 2D electric quadrupole trap with zero along the x-axis. This is shown for the $x = 0$ plane (c), with yellow pins artificially projected for clarity since they don't actually intersect the plane. The central pins are magnetized, with two domains each. Blue indicates magnetization along $+\hat{y}$, red along $-\hat{y}$. These domains produce a magnetic quadrupole trap with zero along the z-axis, shown in the $z = 0$ plane (d).

previous work [43], where electric fields were applied to study collisions. The mechanism of molecular spin-flip loss was identified, and an attempt was made to deconvolve it from the collisional effect of the electric field. Revisiting this with the direct integration of flux, we find a three-fold larger loss magnitude, enough to explain a significant portion of the effect previously attributed to collisions, see Sec. A of the Supplementary [50]. In light of this, it becomes especially important to perform direct, unconvolved experimental verification of both the magnitude of the loss effect and the validity of our loss-flux calculations. We now present the new trap where this is achieved.

Our idea is to use a pair of 2D quadrupole traps, one magnetic and the other electric, with orthogonal centerlines (Fig. 2):

$$\vec{B} = B'x\hat{y} - B'y\hat{x} \qquad \vec{E} = E'y\hat{y} - E'z\hat{z} \tag{4}$$

We achieve these fields in a geometry that matches our Stark decelerator [24]. This geometry features large spin-flip loss, since $\vec{E} \perp \vec{B}$ in both the $x = 0$ and $y = 0$ planes, and from Eqn. 1, $G = \mathcal{B}_\perp^3 \Delta^2 / \mathcal{E}^4$ will be generally very small due to the large $\mathcal{E}$. However, by adding a small magnetic field $\vec{B} = B_{\text{coil}}\hat{z}$ along the centerline of the magnetic quadrupole with an external bias coil, a dramatic change can be made to the surfaces where $\vec{E} \perp \vec{B}$ with minimal perturbation of the trapping potential.

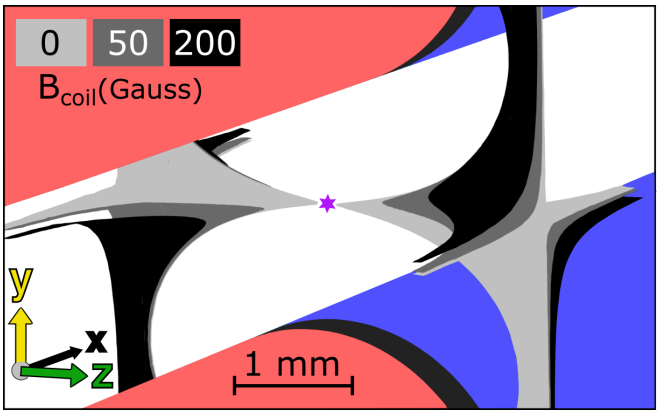

FIG. 3. Surfaces where spin-flips can occur are shown for three values of B_{coil} in light gray, dark gray, and black. The magnetic pins are shown as in Fig. 2 for context. The purple star marks the trap center, to which molecules are confined within a ~1 mm diameter.

B_{coil} morphs the $\vec{E} \perp \vec{B}$ surface from a pair of planes into the hyperbolic sheet given by $x \cdot y = z \cdot B_{\text{coil}}/B'$ (Substitute Eqn. 4 into $\vec{E} \cdot \vec{B} = 0$). This means that $\vec{E} \perp \vec{B}$ is pushed away from the z-axis where $\vec{B}$ is smallest. In Fig. 3, the surfaces where $\vec{E} \perp \vec{B}$ for several B_{coil} magnitudes are calculated and shown wherever $G \leq \kappa$. The loss regions ought to be tuned far enough from the trap center that molecules cannot access them. This is indeed what we observe, note the striking difference in trap lifetimes in Fig. 4a. With only 200 G bias field (the trap is 5 kG deep) the loss is suppressed below that due to background gas.

To further verify our understandings of the loss mechanism, we translated one of the magnetic pins along $\hat{x}$. This pin translation disrupts the idealized 2D magnetic quadrupole by adding a small trapping field $\vec{B} \propto B'z\hat{z}$, which significantly alters the topology of the $\vec{E} \perp \vec{B}$ surface and the overall loss rate in the trap. We also compute loss rates for all values of pin translation and B_{coil} by numerically integrating the loss flux through these unusual loss surfaces via the Landau-Zener formula, just as for the simpler quadrupole geometry discussed previously. The calculated populations after 30 ms in the trap have a reasonable agreement with the measurements (Fig. 4b). The direct integral calculation uses only the temperature of a purely thermal distribution as a free parameter, and does not involve computation of any trajectories. The temperature fits to 170 ± 20 mK [51]. An intuitive explanation for the intriguing double well structure in Fig. 1 is that B_{coil} first translates the magnetic zero along the z-axis, overlapping it with larger electric fields at first before moving it out of the trap.

With strong experimental confirmation of the molecular spin-flip loss enhancement, we can move on to generalize beyond OH. Hund's case (a) states are most susceptible in the sense that smaller electric fields are sufficient

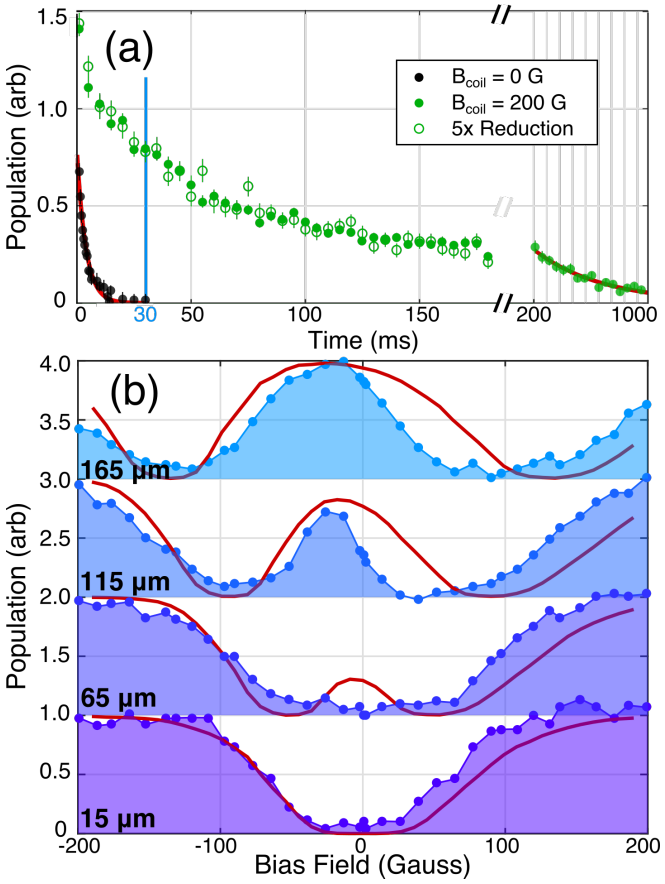

FIG. 4. Time traces (a) without bias field (black), with bias field (green dots), and with modulated density (green circles). One body fits (red) give loss rates of 200 s^{-1} without bias field and 2 s^{-1} with full bias field at long times, in agreement with our background gas pressure. At the fixed time 30 ms, population is shown as a function of both pin translation and bias field (b), for several values of pin translation, labeled relative to perfect alignment. Fits (red) are calculated by integrating the molecule flux of a thermal ensemble through surfaces where $\vec{E} \perp \vec{B}$.

to cause a significant problem, but with enough electric field any state exhibiting competition between electric and magnetic fields for alignment of the molecule or atom will be susceptible. One way to avoid competition is for the fields to couple to unrelated parts of the Hamiltonian, which happens to a limited extent for Hund's case (b) states without electron orbital angular momentum (Σ states, $\Lambda = 0$) [46]. In these states, which include most laser-cooled molecules thus far, the electric and magnetic fields couple to rotation and spin respectively, which are only related by the spin-rotation coupling constant. This constant is usually in the tens of MHz [36], so molecular spin-flip loss remains quite significant. The inclusion of hyperfine requires a careful case-by-case investigation. For OH, it would initially seem to add an extra splitting that could protect from spin-flips, but in fact the loss plane is only shifted slightly away from $\vec{E} \perp \vec{B}$ and retains the same area. For YO [52], certain hyperfine states can avoid spin-flip loss entirely when electric fields are applied. These states are characterized by significant electron-spin-to-nuclear-spin dipolar coupling, which results in a protective gap regardless of field orientation.

It is also instructive to consider the related case of a pure electrostatic trap. Here there is always some zero field parity splitting that prevents the orientation-reversing spin flips we have been discussing. However, this same splitting pushes all states with the same sign of m, the field alignment quantum number, very close to one another, leading to loss via Landau-Zener transitions other than the m to $-m$ spin-flip [53]. Intriguingly, the addition of a homogeneous magnetic field can actually suppress this loss [54].

The present trap, in addition to providing the desired experimental testing ground for molecular spin-flip loss, produces large 5 T/cm trap gradients useful for maintaining high densities to facilitate collisional studies. This is in contrast with other strategies for plugging the hole of a magnetic trap which often lead to a reduction in trap gradient. With loss removed, we observe a population trend whose initially fast decay rate decreases over time (Fig. 4a, green dots), suggesting a two-body collisional effect. We test this by reducing the initial population fivefold but without changing its spatial or velocity distribution [50], and then scale the resulting trend by five (green circles). If collisions had contributed, this new trend would show less decay, but we observe no significant change. This seeming lack of collisions is likely due to the much higher initial temperature of 170 mK, in contrast to the earlier work at and below 50 mK [35]. An alternative hypothesis for the population trend is the existence of chaotic trap orbits with long escape times [55]. The understanding of electric field enhanced spin-flip loss brings an important consequence to the use of RF knife under electric field employed in the forced evaporation, especially at low temperatures. We present the effect of evaporation at intermediate temperatures ($\sim$30 mK) in Sec. B of the Supplementary [50]. Moving forward, we aim to increase the density by means of several improvements [56, 57].

Molecule enhanced spin-flip loss arises in mixed electric and magnetic fields due to a competition between field quantization axes. We conclusively demonstrate and suppress this effect using our dual magnetic and electric quadrupole trap, which is also an ideal setting for further progress in collisional physics thanks to its large trap gradient. Our calculation of the magnitude of spin-flip loss via flux through surfaces where $\vec{E} \perp \vec{B}$ enables detailed predictions of how its location and magnitude ought to scale with bias field and trap alignment, which we experimentally verify. Our results correct existing predictions about molecular spin-flips in mixed fields and pave the way toward further improvements in molecule trapping and cooling.

We acknowledge the Gordon and Betty Moore Foundation, the ARO-MURI, JILA PFC, and NIST for their financial support. T.L. acknowledges support from the Alexander von Humboldt Foundation through a Feodor Lynen Fellowship. We thank J.L. Bohn, S.Y.T. van de Meerakker, and M.T. Hummon for helpful discussions. We thank Goulven Quéméner for his continued involvement in this research.

* Contributed equally. Email dave.reens@colorado.edu or hao.wu@colorado.edu.

† Present Address: 5. Physikalisches Institut and Center for Integrated Quantum Science and Technology (IQST), Universität Stuttgart, Pfaffenwaldring 57, 70569 Stuttgart, Germany

[1] L. D. Carr, D. DeMille, R. V. Krems, and J. Ye, New Journal of Physics **11**, 055049 (2009).

[2] M. Greiner, C. A. Regal, and D. S. Jin, Nature **426**, 537 (2003).

[3] M. W. Zwierlein, C. A. Stan, C. H. Schunck, S. M. F. Raupach, S. Gupta, Z. Hadzibabic, and W. Ketterle, Physical Review Letters **91**, 250401 (2003).

[4] S. Jochim, M. Bartenstein, A. Altmeyer, G. Hendl, S. Riedl, J. Hecker Denschlag, and R. Grimm, Science **302**, 2101 (2003).

[5] T. Bourdel, L. Khaykovich, J. Cubizolles, J. Zhang, F. Chevy, M. Teichmann, L. Tarruell, S. J. J. M. F. Kokkelmans, and C. Salomon, Physical Review Letters **93**, 050401 (2004).

[6] K.-K. Ni, S. Ospelkaus, M. H. G. de Miranda, A. Pe'er, B. Neyenhuis, J. J. Zirbel, S. Kotochigova, P. S. Julienne, D. S. Jin, and J. Ye, Science **322**, 231 (2008).

[7] J. G. Danzl, M. J. Mark, E. Haller, M. Gustavsson, R. Hart, J. Aldegunde, J. M. Hutson, and H.-C. Nägerl, Nature Physics **6**, 265 (2010).

[8] T. Takekoshi, L. Reichsöllner, A. Schindewolf, J. M. Hutson, C. R. Le Sueur, O. Dulieu, F. Ferlaino, R. Grimm, and H.-C. Nägerl, Physical Review Letters **113**, 205301 (2014).

[9] P. K. Molony, P. D. Gregory, Z. Ji, B. Lu, M. P. Köppinger, C. R. Le Sueur, C. L. Blackley, J. M. Hutson, and S. L. Cornish, Physical Review Letters **113**, 255301 (2014).

[10] J. W. Park, S. A. Will, and M. W. Zwierlein, Physical Review Letters **114**, 205302 (2015).

[11] M. Guo, B. Zhu, B. Lu, X. Ye, F. Wang, R. Vexiau, N. Bouloufa-Maafa, G. Quéméner, O. Dulieu, and D. Wang, Physical Review Letters **116**, 205303 (2016).

[12] B. Drews, M. Deiß, K. Jachymski, Z. Idziaszek, and J. Hecker Denschlag, Nature Communications **8**, 14854 (2017).

[13] L. R. Liu, J. T. Zhang, Y. Yu, N. R. Hutzler, Y. Liu, T. Rosenband, and K.-K. Ni, ArXiv:1701.03121 , 1.

[14] T. M. Rvachov, H. Son, A. T. Sommer, S. Ebadi, J. J. Park, M. W. Zwierlein, W. Ketterle, and A. O. Jamison, Journal of Physics B: Atomic and Molecular Physics **3**, 1620 (2017).

[15] S. A. Moses, J. P. Covey, M. T. Miecnikowski, B. Yan, B. Gadway, J. Ye, and D. S. Jin, Science **350**, 659 (2015).

[16] B. K. Stuhl, B. C. Sawyer, D. Wang, and J. Ye, Physical Review Letters **101**, 243002 (2008).

[17] M. T. Hummon, M. Yeo, B. K. Stuhl, A. L. Collopy, Y. Xia, and J. Ye, Physical Review Letters **110**, 143001 (2013).

[18] J. F. Barry, D. J. McCarron, E. B. Norrgard, M. H. Steinecker, and D. DeMille, Nature **512**, 286 (2014).

[19] V. Zhelyazkova, A. Cournol, T. E. Wall, A. Matsushima, J. J. Hudson, E. A. Hinds, M. R. Tarbutt, and B. E. Sauer, Physical Review A **89**, 053416 (2014).

[20] B. Hemmerling, E. Chae, A. Ravi, L. Anderegg, G. K. Drayna, N. R. Hutzler, A. L. Collopy, J. Ye, W. Ketterle, and J. M. Doyle, Journal of Physics B: Atomic, Molecular and Optical Physics **49**, 174001 (2016).

[21] S. Truppe, H. J. Williams, M. Hambach, L. Caldwell, N. J. Fitch, E. A. Hinds, B. E. Sauer, and M. R. Tarbutt, Nature Physics (2017).

[22] J. D. Weinstein, R. DeCarvalho, T. Guillet, B. Friedrich, and J. M. Doyle, Nature **395**, 148 (1998).

[23] H. L. Bethlem, G. Berden, and G. Meijer, Physical Review Letters **83**, 1558 (1999).

[24] J. R. Bochinski, E. R. Hudson, H. J. Lewandowski, G. Meijer, and J. Ye, Physical Review Letters **91**, 243001 (2003).

[25] E. Narevicius, A. Libson, C. G. Parthey, I. Chavez, J. Narevicius, U. Even, and M. G. Raizen, Physical Review Letters **100**, 093003 (2008).

[26] A. Wiederkehr, H. Schmutz, M. Motsch, and F. Merkt, Molecular Physics **110**, 1807 (2012).

[27] S. Marx, D. Adu Smith, G. Insero, S. A. Meek, B. G. Sartakov, G. Meijer, and G. Santambrogio, Physical Review A **92**, 063408 (2015).

[28] A. Prehn, M. Ibrügger, R. Glöckner, G. Rempe, and M. Zeppenfeld, Physical Review Letters **116**, 063005 (2016).

[29] Y. Liu, M. Vashishta, P. Djuricanin, S. Zhou, W. Zhong, T. Mittertreiner, D. Carty, and T. Momose, Physical Review Letters **118**, 093201 (2017).

[30] B. C. Sawyer, B. K. Stuhl, M. Yeo, T. V. Tscherbul, M. T. Hummon, Y. Xia, J. Kłos, D. Patterson, J. M. Doyle, and J. Ye, Physical Chemistry Chemical Physics **13**, 19059 (2011).

[31] A. von Zastrow, J. Onvlee, S. N. Vogels, G. C. Groenenboom, A. van der Avoird, and S. Y. T. van de Meerakker, Nature Chemistry **6**, 216 (2014).

[32] A. Klein, Y. Shagam, W. Skomorowski, P. S. Żuchowski, M. Pawlak, L. M. C. Janssen, N. Moiseyev, S. Y. T. van de Meerakker, A. van der Avoird, C. P. Koch, and E. Narevicius, Nature Physics **13**, 35 (2016).

[33] X. Wu, T. Gantner, M. Koller, M. Zeppenfeld, S. Chervenkov, and G. Rempe, Science , 10.1126/science.aan3029 (2017).

[34] L. P. Parazzoli, N. J. Fitch, P. S. Żuchowski, J. M. Hutson, and H. J. Lewandowski, Physical Review Letters **106**, 193201 (2011).

[35] B. K. Stuhl, M. T. Hummon, M. Yeo, G. Quéméner, J. L. Bohn, and J. Ye, Nature **492**, 396 (2012).

[36] G. Quéméner and J. L. Bohn, Physical Review A **93**, 012704 (2016).

[37] W. Petrich, M. H. Anderson, J. R. Ensher, and E. A. Cornell, Physical Review Letters **74**, 3352 (1995).

[38] K. B. Davis, M. O. Mewes, M. R. Andrews, N. J. van Druten, D. S. Durfee, D. M. Kurn, and W. Ketterle,

Physical Review Letters **75**, 3969 (1995).
[39] B. C. Sawyer, B. K. Stuhl, D. Wang, M. Yeo, and J. Ye, Physical Review Letters **101**, 203203 (2008).
[40] J. Riedel, S. Hoekstra, W. Jäger, J. J. Gilijamse, S. Y. T. Van De Meerakker, and G. Meijer, European Physical Journal D **65**, 161 (2011).
[41] M. Quintero-Pérez, T. E. Wall, S. Hoekstra, and H. L. Bethlem, Journal of Molecular Spectroscopy **300**, 112 (2014).
[42] N. Akerman, M. Karpov, Y. Segev, N. Bibelnik, J. Narevicius, and E. Narevicius, Physical Review Letters **119**, 073204 (2017).
[43] B. K. Stuhl, M. Yeo, M. T. Hummon, and J. Ye, Molecular Physics **111**, 1798 (2013).
[44] B. K. Stuhl, M. Yeo, B. C. Sawyer, M. T. Hummon, and J. Ye, Physical Review A **85**, 033427 (2012).
[45] M. Lara, B. L. Lev, and J. L. Bohn, Physical Review A **78**, 033433 (2008).
[46] J. L. Bohn and G. Quéméner, Molecular Physics **111**, 1931 (2013).
[47] The authors use $\mu_{\text{eff}}\vec{B} \pm d_{\text{eff}}\vec{E}$. We reverse this to provide a more physical connection to our experiment, where the electric field is fixed.
[48] M. A. Player and P. G. H. Sandars, Journal of Physics B: Atomic and Molecular Physics **3**, 1620 (1970).
[49] J. J. Hudson, B. E. Sauer, M. R. Tarbutt, and E. A. Hinds, Physical Review Letters **89**, 023003 (2002).
[50] See Supplementary Materials.
[51] Calculation performed in COMSOL: Source Code.
[52] This is particularly relevant given the recently realized 3D MOT for YO.
[53] T. E. Wall, S. K. Tokunaga, E. a. Hinds, and M. R. Tarbutt, Physical Review A **81**, 033414 (2010).
[54] S. A. Meek, G. Santambrogio, B. G. Sartakov, H. Conrad, and G. Meijer, Physical Review A **83**, 033413 (2011).
[55] R. González-Férez, M. Iñarrea, J. P. Salas, and P. Schmelcher, Physical Review E **90**, 062919 (2014).
[56] U. Even, EPJ Techniques and Instrumentation **2**, 17 (2015).
[57] Y. Segev, N. Bibelnik, N. Akerman, Y. Shagam, A. Luski, M. Karpov, J. Narevicius, and E. Narevicius, Science Advances **3**, e1602258 (2017).